

Introduction

- Tissues of the intervertebral disc: nucleus pulposus (NP), annulus fibrosus (AF), and cartilaginous endplates (CEPs), consists mainly of water and proteoglycans (GAGs) and healthy NP and AF have an excellent swelling capacity (>50%) [1, 2].
- Previous studies showed that AF swelling is anisotropic and dependent on fiber architecture (*i.e.*, fiber angle and lamellae) [2, 3]. Moreover, annular ring geometry affects swelling by forming compressive stress/strain in the inner layers and tensile stress/strain in the outer layers [4-6].
- However, these studies have not evaluated disc joint swelling. *Thus, interactions between disc subcomponents during swelling are not well understood.*
- Native disc degeneration has been noted with large decreases in GAG content and intradiscal pressure, particularly in the NP and inner AF [7-8].
- Our previous work simulated AF swelling by describing the AF structure as a stand-alone ring structure. We showed that GAG loss in the inner AF decreased swelling ratio and circumferential-direction stress by more than 50% [6].
- Therefore, the objective of the current study was to **1) evaluate the interactions between disc subcomponents under swelling conditions**, and **2) evaluate the effect of step-wise GAG loss on disc swelling behavior.**

Method

Geometry

- 5 models were created: NP explant, CEP explant, AF ring (20 layers), NP with AF (NP+AF), and intact disc (Fig. 1).

Material description

- Triphasic mixture theory was used to describe tissues as a combination of three phases: a solid phase and two fluid phases (water and monovalent ions) [9].
- Solid phase was Holmes-Mow compressible hyperelastic material, while AF solid phase had an additional component for nonlinear fibers [10].
- Degeneration was simulated by altering GAG distribution through the Fixed-charge density (FCD; degeneration levels 1-3).
- 18 model simulations were run and compared (Tab. 1&2).
- All material parameters were chosen from literature [6,11].

Load conditions

- Steady-state swelling was simulated in FEBio by increasing FCD from zero to the specified value, while surrounding environment remained constant. Swelling-ratio (SR) was calculated as the volume after swelling divided by initial volume.

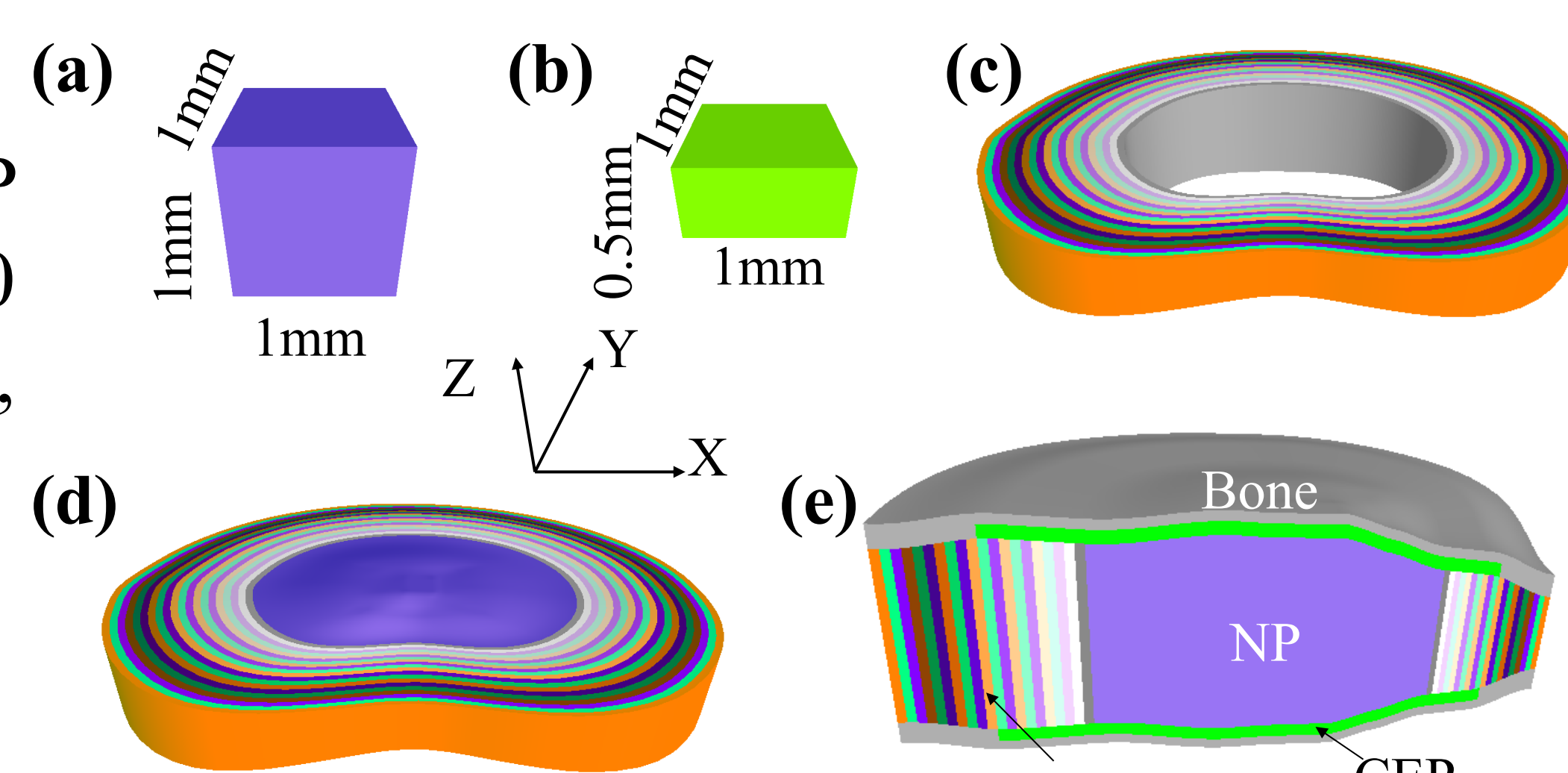


Fig. 1. Models: (a) NP explant, (b) CEP explant, (c) AF, (d) NP + AF, (e) Disc (mid sagittal view).

| Disc (D) | NP+AF | NP explant (NP) | CEP explant (CEP) | AF ring (AF) |
|-------------|-------|-----------------|-------------------|--------------|
| Healthy (H) | H | H | H | H&L1 |
| Level1 (L1) | L1 | L1 | L1 | |
| Level2 (L2) | L2 | L2 | L2 | L2&L3 |
| Level3 (L3) | L3 | L3 | L3 | |

Table 1. 18 models represent disc and its subcomponents at different levels of degeneration.

| | Healthy | Level 1 | Level 2 | Level 3 |
|-----|-------------|---------|-------------|---------|
| NP | -400 | -300 | -150 | -100 |
| CEP | -124 | -90 | -45 | -30 |
| AF* | -300 (-100) | | -150 (-100) | |

Table 2. FCD (mmol/L) for healthy and three levels/degrees of degeneration [7-8]. *FCD magnitude decreased linearly from inner AF to outer (values in parentheses).

Acknowledgements

This study was supported by the National Science Foundation (NSF CAREER, 1751212).

Email: g.oconnell@berkeley.edu, web: oconnell.berkeley.edu

Results

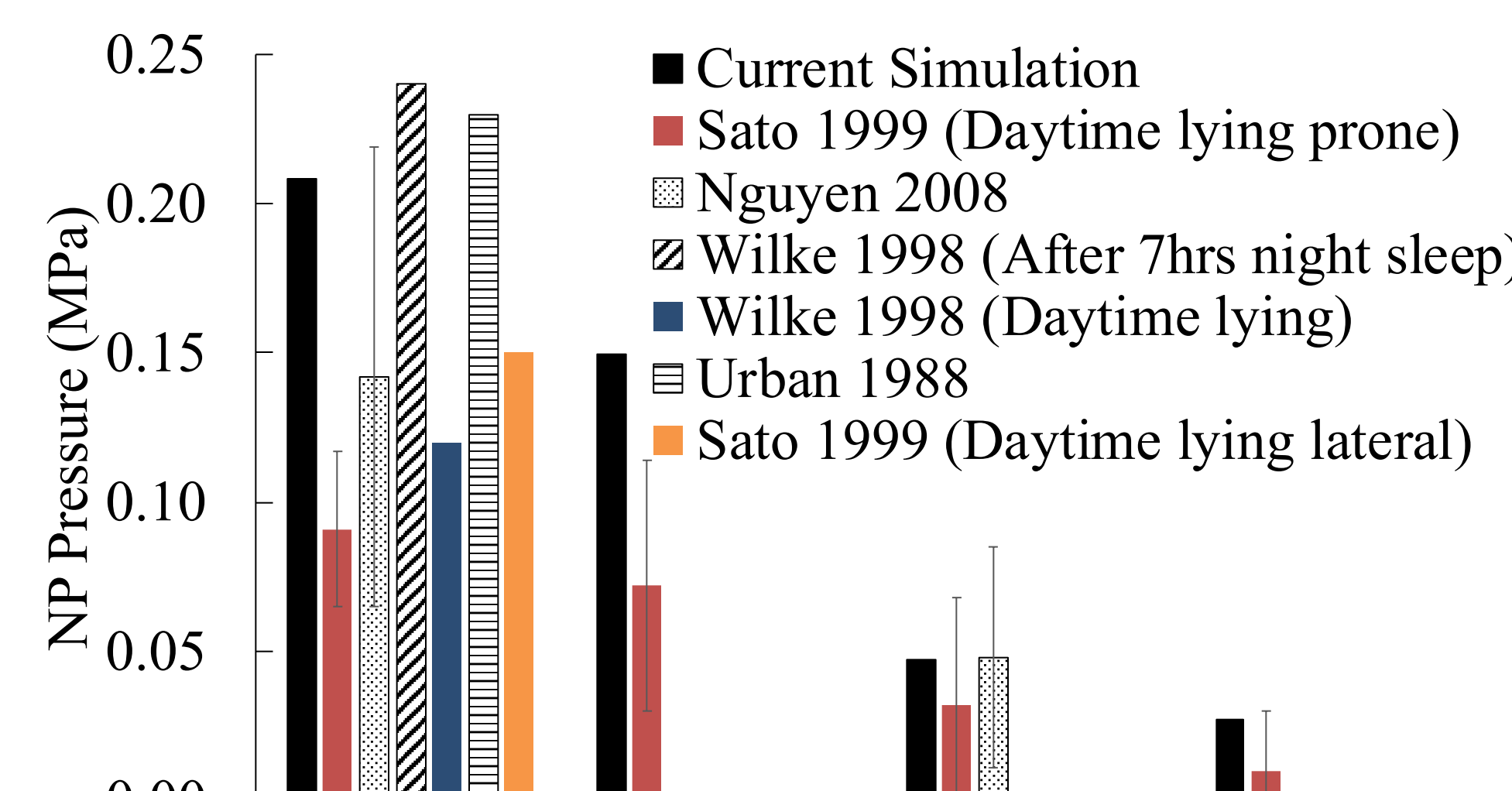


Fig. 2: Swelling-based residual pressure in NP compared to values in the literature [12-15].

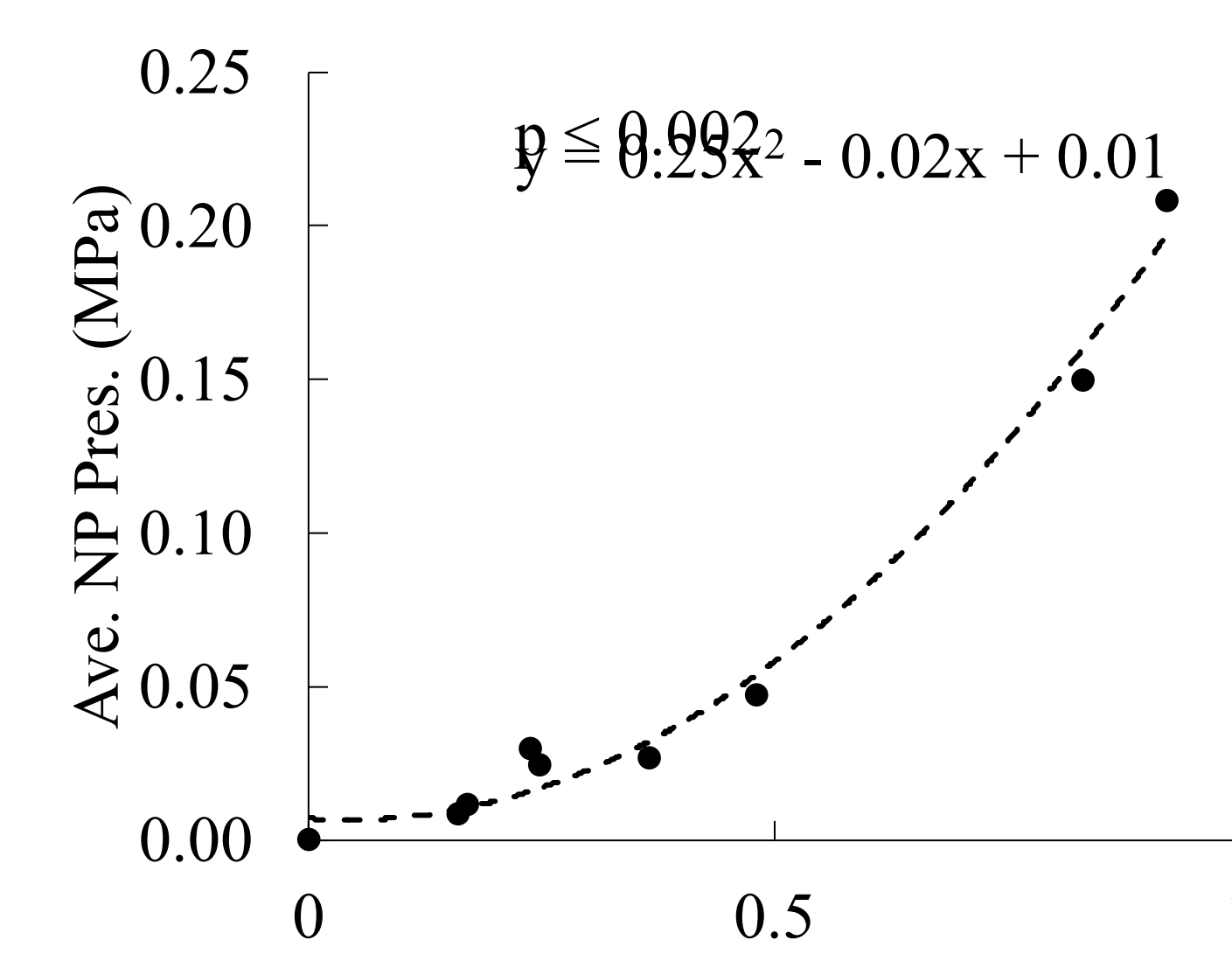


Fig. 4: NP pressure in intact disc vs. NP explant SR subtracted by NP SR in situ

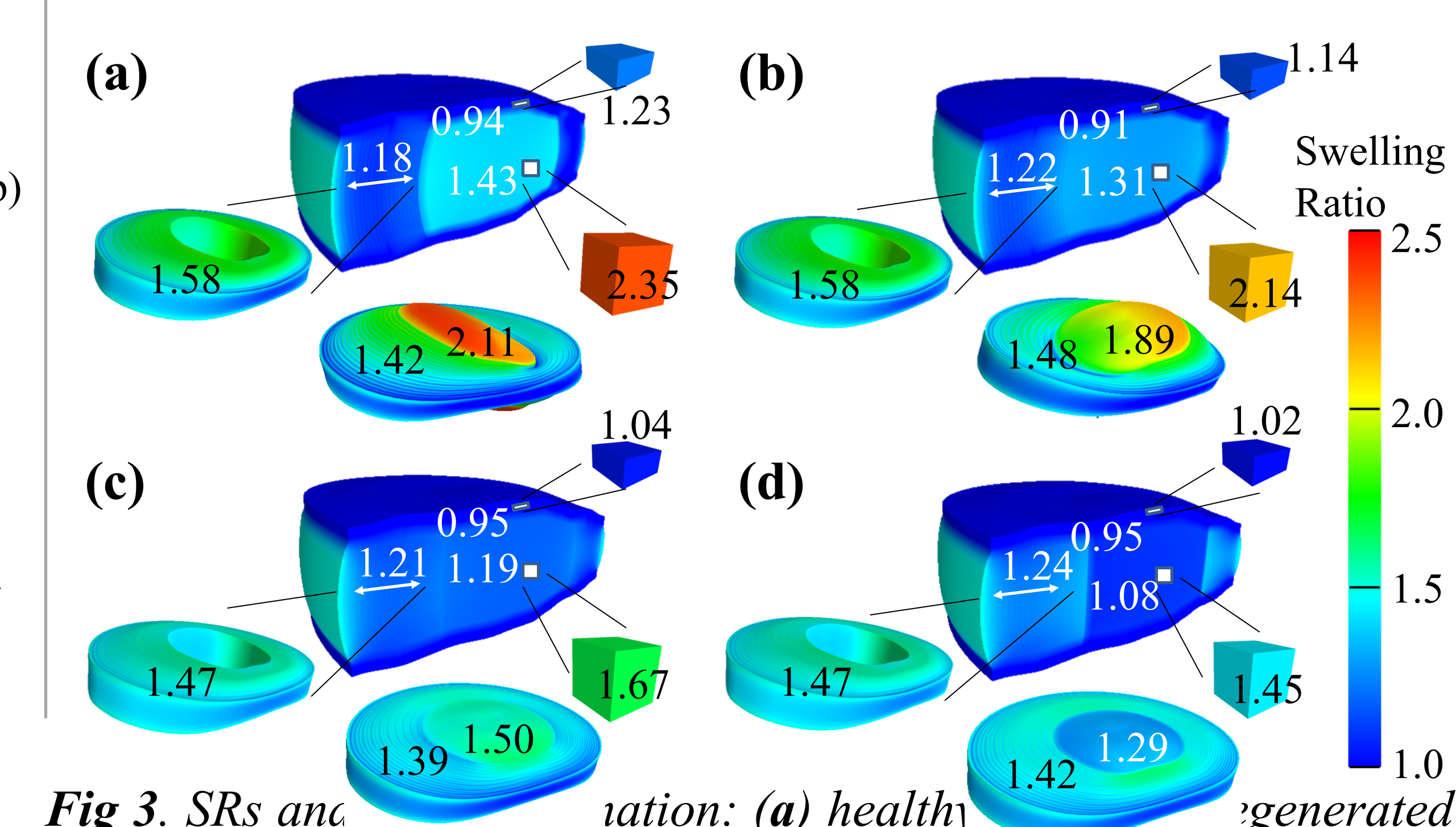


Fig. 3. SRs and distribution: (a) healthy, (b) degenerated (levels 1-3) discs. Values represent SR for each subcomponent.

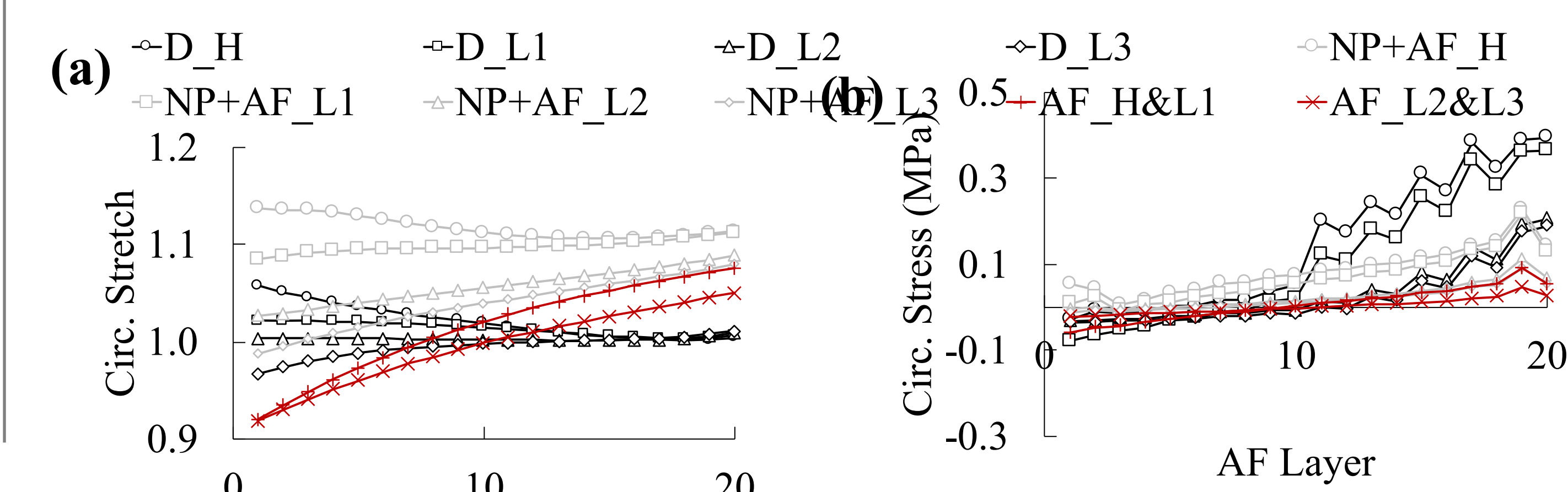


Fig. 5: Layer-averaged circumferential (a) stretch and (b) stress of annulus fibrosus in Disc, NP+AF, and AF models at different health status.

- NP pressure agreed with experimental data in the literature (Fig. 2).
- As expected, tissue swelling decreased with additional boundary constraints, such that NP swelling *in situ* was 40% lower than the NP explant and AF swelling *in situ* was 20% lower than the AF ring (Fig. 3).
- Although the inner AF GAG decreased with degeneration, *in situ* AF swelling ratio increased (Fig. 3)
- A nonlinear relationship between NP pressure of the intact disc was observed with the SR of NP explant subtracted by *in situ* SR (Fig 4).
- Circumferential stretch of the inner AF was more influenced by physiological boundary condition (Fig. 4a – red & grey lines) and degeneration than the outer layers (Fig. 4a – black lines).
- Tensile stress in the outer AF decreased with degeneration in the NP and inner AF (Fig. 5b - black lines).

Discussion

- We developed models for the disc and its subcomponents to evaluate interactions between subcomponents during swelling and to evaluate the effect of GAG loss in the NP and inner AF on overall disc swelling behavior.
- Degeneration decreased tissue swelling capacity for all tissues, however, ***in situ swelling of the AF and CEP increased with degeneration due to larger relative decreases in NP swelling ratio.***
- Similar to previous observations with arterial walls [4-6], ***development of compressive stretch in the AF with swelling was important for maintaining uniform stretch*** once an internal pressure is applied by the NP (Fig. 5a – red versus black lines).
- The relationship between intradiscal pressure and NP explant SR subtracted by the *in situ* NP SR (Fig. 4) highlights the importance of replicate NP swelling capability in biological repair strategies [16].
- In conclusion, NP, AF, and endplates restrict each other during *in situ* swelling: Suppression of NP swelling resulted in an increase in intradiscal pressure in the healthy disc, and degeneration has a significant impact on subcomponent swelling.

References

- [1] Bezci, SE + J Biomech Eng 137.10: 101007, 2015; [2] Žak, M + Eur. Spine J. 25(9):2681-90 2016; [3] Yang, B + J Mech Behav Biomed 82:320-8. 2018; [4] Michalek, AJ + J Biomech.;45(7):1227-31. 2012; [5] Duclos, SE + J Mech Behav Biomed. 68:232-8, 2017; [6] Yang, B + Biomech Model Mechanobiol 2018; [7] Antoniou, J + J Clin Invest. 98(4):996-1003. 1996; [8] Wu, Y + Spine. 42(17): E1002-9. 2017; [9] Lai, WM + J Biomech Eng., 113(3):245-58,1991; [10] Yang, B + Biomech Model Mechanobiol 16(6):2005-15. 2017; [11] Cortes, DH + J Biomech. 47(9):2088-94. 2014; [12] Sato, K + Spine. 24(23):2468. 1999; [13] Nguyen, AM + J Bone Joint Surg 90(4):796. 2008; [14] Wilke, HJ + Clin Biomech 16:S111-26. 2001; [15] Urban, JP, + Spine. 13(2):179-87. 1988 ; [16] Sivan, SS + Eur Spine J 23:S344–53 2014.